

NOTICE WARNING CONCERNING COPYRIGHT RESTRICTIONS:

The copyright law of the United States (title 17, U.S. Code) governs the making of photocopies or other reproductions of copyrighted material. Any copying of this document without permission of its author may be prohibited by law.

**A Unified Approach for the Simultaneous
Synthesis of Reaction, Energy and Separation Systems**

S. Balakrishna, L. Biegler

EDRC 06-156-93

A Unified Approach for the Simultaneous Synthesis of Reaction, Energy and Separation Systems

*5. Balakrishna and L.T. Biegler**
Department of Chemical Engineering
Carnegie Mellon University
Pittsburgh, PA 15213

Revised for I & EC Research
March, 1993

*** Author to whom correspondence should be addressed**

ABSTRACT

Previous studies on process integration have generally considered reaction and separation as processes that occur sequentially in a flowsheet. In this paper, a unified formalism is presented for the synthesis of reaction-separation systems, while ensuring "optimal" energy management. The synthesis model stems from a target-based approach for reactor networks due to an earlier study. It is shown that by postulating a species dependent residence time distribution function, one can arrive at a general representation for a reaction-separation network. Optimization of this distribution function leads to a separation profile as a function of time along the length of the reactor. The synthesis model is formulated as a mixed integer optimal control problem, where the integer variables account for the fixed costs of separation. The control profiles include the temperature, the separation profile, and residence time distribution defined for the network. Costs for maintaining a separation profile are handled through a separation index (defined to model the intensity of separation), and a fixed charge for any separation between two components in the reaction mixture. Also, using an energy targeting formulation, the maintenance of the optimal temperature profile is integrated to the energy flows within the flowsheet. Strategies based on simultaneous optimization and model solution are presented for the optimization problem and demonstrated for two case studies.

1. Introduction

Decomposition techniques for chemical engineering systems are largely based on the concept of unit operations. These provide a natural scheme for classifying the physical phenomena occurring in the different subsystems, thereby reducing significantly the complexity for analysis of these systems. At the same time, however, this decomposition has also shadowed to some extent the amalgamation of the various physical phenomena represented by the respective unit operations. The integration of the synthesis schemes developed for different subsystems (for example, reactors, energy networks, and separation systems) has recently received substantial attention. Notable among these are the conceptual design ideas of Douglas (1988), and the schemes based on the idea of hierarchical decomposition (Douglas, 1985,1989; Glavic et al., 1988). On the other hand, by assuming distillation based sharp splits, Piboleau and Roquet (1988) developed mixed integer programming formulations to optimize reactor-separator performance* Floudas et al. (1989) extended their mixed integer nonlinear programming formulation for reactor synthesis to include reactor, separator and recycle units. Despite the insights that have resulted from these efforts, a major limitation stems from the fact that they currently do not allow the combination of various physical phenomena in different subsystems. For example, the above approaches do not consider the synthesis of novel schemes such as simultaneous reactive separation processes within their framework.

In this paper, we aim to develop a targeting scheme with a capability to simultaneously assess the importance of reaction, mixing, separation, and heat exchange on overall performance. The synthesis approach is developed in the light of the ideas previously presented on the sequential bounding scheme for reactor targeting (Balakrishna and Biegler, 1992 a,b). By considering the reactor as the main unit of the chemical plant, we develop formulations to derive a reactor network that performs optimally in conjunction with the separation and energy network. While previous formulations have considered reaction and separation as sequential operations in a flowsheet, our model is developed to consider simultaneous reaction and separation as an option within the network.

In the next section, we develop a non-isothermal reactor model, which allows for separation as reaction progresses. This is facilitated through a special choice of

residence time distribution. Optimization of this residence time distribution function leads to a separation profile as a function of age. Following this, we consider the amalgamation of this formulation with energy minimization and develop simplifications for systems with highly exothermic reactions. The solution to this model gives us a lower bound on the performance index; and schemes to successively improve these bounds are presented. These ideas are demonstrated on two example problems, and the results indicate significantly better overall performance, when all the subsystems are considered simultaneously. Particularly, the influence of separation in the course of reaction seems to play an important role in overall performance.

2. Model Formulation : Combined Reaction-Separation Model

Figure 1 below shows a schematic of a simultaneous reaction - separation model. In a reactor targeting model to include separation, we essentially postulate an age based separation function vector (y) in the same spirit as a residence time distribution function for homogeneous reactors. However, here each species has its own residence time distribution function dependent on its separation function y_c . Also, X_0 is the mass concentration of feed entering the reactor network, a is the independent variable denoting the age of a molecule as it progresses along the length of the reactor. Q_0 is the flow rate at the entrance of the network and $m_c(a)$ is the mass of component c in the reactor at age a . We define a separation function $y_c(a)$ such that between age a and $a + 5a$, a mass fraction of species c equivalent to $Y_c(a)5a$ leaves the reactor.

Hence,

$$\frac{dP^*}{da} = -y_c(a)mc(a) + R(X,T)Q(a) \quad (1)$$

where

$m_c(a)$: Mass flow of species c at age a ($c = 1, C$)

$Q(a)$: Volumetric flow rate at age a

$X(a)$: Mass concentration vector

$m(a)$: Mass flow vector (Array of n^{\wedge})

$R(X,T)$: Reaction Rate Vector

For a homogenous system, if p is the density of the system, then,

$$\frac{dS}{da} = \sum_c \frac{V_c(oc)mc(oc)}{p} \quad (2)$$

We assume constant density systems for the sake of simplicity , even though variable density could be considered by a straightforward extension to this model.

Consider an infinitesimal element $5a$ in the reactor-separator configuration above, where,

- $X_c(a)$: Mass Concentration of species c at age a
 $X_c(a+5a)$: Mass Concentration of species c at age $a + 5a$
 $Y_c(a)$: Vector of separation fractions at age a . (array of $y_c(a)$)

A differential balance around an infinitesimal element $5a$ for component c gives :

$$X_c(a+5a)Q - X_c(a)Q = R_c(X,T)Q(5a) - y_c(a)Q(5a)X_c(a) \quad (3)$$

$$Q(a+5a) = Q(a) \left[1 - \frac{\sum_{c=1}^C y_c(a)X_c(a)}{P} 5a \right] \quad (4)$$

Substituting for $Q(a+5a)$ from (4) in (3), we get,

$$X_c(a+5a)Q(a) \left[1 - \frac{\sum_{c=1}^C Y_c(a)X_c(a)}{P} 5a \right] - X_c(a)Q(a) = R_c(X,T)Q(5a) - Y_c(a)Q(5a)X_c(a)$$

or

$$[X_c(a+5a) - X_c(a)]/5a - X_c(a+5a) \frac{\sum_{c=1}^C Y_c(a)X_c(a)}{P} = R_c(X,T) - Y_c(a)X_c(a)$$

Taking the limit as $5a$ tends to zero, we have:

$$\frac{dX_c}{da} = R_c(X, T) + X_c(a) \left[\frac{Y_c(a)}{p} - r_c(a) \right] \quad (5)$$

With this governing equation, a mathematical model (PI) for maximizing the performance index in this reacting environment can be derived as follows:

$$\text{Max}_{y, T} \quad J_{\text{exit}}(m_c(\text{exit}), Q, X) \quad (\text{PI})$$

$$\frac{d}{da} = R_c(X, T) + X_c(a) \left[\frac{Y_c(a)}{p} - r_c(a) \right]; \quad c = 1, C$$

$$\frac{dQ}{da} = - \sum_{c=1}^C \frac{\gamma_c(a) m_c(a)}{p}$$

$$m(a) = X(a)Q(a)$$

$$m_c(0) = m_{c0} \quad (6)$$

$$\sum_{c=1}^C m_c(0) = \sum_{c=1}^C m_c(\text{exit}) \quad (7)$$

$$m_c(\text{exit}) = \int_0^{\infty} Y_c(a) m_c(a) da \quad (8)$$

$$X = \int_0^{\infty} f(a) da \quad (9)$$

$$g(y, X, i) \geq 0 \quad (10)$$

$$h(y, X, n) = 0 \quad (11)$$

Here, J is an objective function specified by the designer, $X(a)$ is the mass concentration vector of molecules of age a . $m_c(0)$ is the mass flow of each species at the entrance to the reactor, $m_c(\text{exit})$ is the mass flow of each species at the reactor exit given

as the integral of outlet flows at different points within the reacting system, x , the residence time, is determined from the RTD function f for the system as shown in Equation (13) below. The derivation of the actual RTD function for this system in terms of the Y_s is relegated to the appendix. Also, g and h represent the inequality and equality constraints imposed by the environment variables (j_i) on the reaction system.

Clearly, the above formulation is an optimal control problem with differential equation constraints, where the Y_c 's, and the temperature are the control profiles. The solution to this model will give us the optimal separation profile along the reactor. It is clear that the second term in Equation (5) models the effect of separation within the reactor network. Furthermore, if we consider in equation (5) that all the elements of the vector $\gamma(\alpha)$ are the same (which implies that there is no relative separation between the species in the reactor), then the second term vanishes, since

$$\gamma(\alpha)^T X(\alpha) = \sum_c \gamma_c X_c = \gamma_c \sum_c X_c = \gamma_c P, \text{ therefore, } \left[\frac{Y_c(a) T X(a)}{P} - Y_c(a) \right] = 0; \forall c \in C$$

Thus, the governing equation to this reactor scheme reduces to that of segregated flow, and the formulation reduces to the segregated flow optimization problem (Balakrishna and Biegler (1992a)). Furthermore, in this case, the y_c can be directly related to the RTD function (Appendix A) through the following relation:

$$\gamma_c(\alpha) = \frac{f(\alpha)}{1-F(\alpha)} \quad (12)$$

where, $f(a)$ is the residence time distribution of the molecules within the reactor network,

$$F(a) \text{ is the cumulative RTD} = \int_0^a f(t) dt$$

However, if the γ_c 's are not the same for all components (c), i.e; there exists a separation profile, then the actual RTD for this system is given by:

$$f(\alpha) = \sum_c \frac{\gamma_c(\alpha) q_c(\alpha)}{Q_0}, \quad (13)$$

where, $q_c(a) = m_c(\alpha)/\rho$.

The solution to the model PI gives us the optimal separation profile as a function of age within the reactor. However, to solve PI as a nonlinear programming problem, some discretization of profiles will be necessary. Moreover, a continuous separation profile may not be implementable in practice. To address this, we take advantage of the structure of a discretization procedure for the differential equation system. In this case, we choose orthogonal collocation on finite elements (Cuthrell and Biegler, 1987) to discretize the above model for the state variables X and Q . This results in a reactor structure as shown in Figures 2a and 2b, where we restrict separation only to the ends of each finite element

Note the differential equations are converted to algebraic equations through collocation, and the optimal control problem is now reduced to the nonlinear program shown below. Furthermore, it can be shown that as $\Delta\tau$ tends to zero, this discretized model is a close approximation to the original optimal control problem; as shown in Appendix B. The $Y_c(\tau)$ in the original model now reduces to a mass split fraction vector of each species at the end of the i^* element (y_{ci}). The control profiles temperature (T) and separation fractions (y_c) (i.e., the degrees of freedom for the optimization problem) are assumed to be piecewise constant within each element, while the state variables are represented as Lagrange polynomials. The solution to this nonlinear program yields the values of Y_c 's at the end of each element, so that we now know the mass split fractions of each component at each separation level.

Let the set $I = \{i\}$ denote the set of finite elements, $\{k\}, \{j\}$ denote the sets of collocation points. The target to the reaction-separation model can then be derived by the solution to the following nonlinear programming problem:

$$\text{Max}_{\gamma, T} \quad J_{\text{exit}}(x_{\text{exit}}) \quad (\text{P2})$$

$$\sum_k X_{ik} L_k'(t_j) / \Delta\tau_{ci} - R(X, T, y) = 0 \quad @ t_j \quad \text{st } j \neq 0 \quad (14)$$

$$X(0) = X_0 \quad (15)$$

$$X_{\text{end}} \wedge X_{\text{fc}} L_k(0_{\text{end}}) \quad (16)$$

$$m_{c4+1} \ll [X_{c, \text{end}}] Q_i [1 - Y_{ci}] \quad (17)$$

$$X_{i0}Q(i) = \text{raj} \quad (18)$$

$$Q_{(i+1)} = Q_i [1 - X_{iend}^T \gamma_i / \rho] \quad (19)$$

$$m_{c,exit} = \sum_i X_{c,iend} \gamma_{c,i} Q_i \quad (20)$$

$$f(i) = \frac{\gamma_i^T m_i}{Q_0} \quad (21)$$

$$\tau = \sum_i f(i) t(i) \leq t_{max} \quad (22)$$

$$\sum_i \Delta \alpha_i = t_{max} \quad (23)$$

where,

X_{ik} : Mass concentration vector at collocation point k in finite element i (point [ij])

$L_k'(t_j)$: Derivative of Lagrange interpolation polynomial at [ij]

Y_i : Mass split fraction vector at the end of finite element i (Array of Y_{ci})

$f(i)$: Actual RTD for the system at element i given by (13)

T_{jj} : Temperature at [ij]

X^d : Mass concentration vector at the end of elements

m_i : Species Mass flow vector entering element i

Q_i : Total Volumetric Flow Rate entering element i

(14) represents the equations of orthogonal collocation applied to the differential equations at the collocation points. $\Delta \alpha_i$ is the length of each finite element. The values for X at an element are extrapolated to find the values X_{iend} at the end of that element through Lagrange interpolation in (16). Equations (17), (18) and (19) represent mass balances at the separation point. The mass flow rate of each species exiting the reactor is shown in (20). The discretized RTD function is given in (21); and the expression for the mean residence time follows in (22). As $\Delta \alpha \rightarrow 0$, this model is equivalent to the original reaction-separation model, PL. The main difference is that we allow separation only at the end of each element; within each element no separation occurs. Though the model appears nonlinear, the nonlinearities are actually reduced when one considers the rates in terms of the mass fractions. The solution to this model then gives us the optimal separation split fractions as a function of age along the reactor.

Note that while the profiles from (P1) may not be straightforward to implement as a practical design, solution of this model requires the discretization given in (P2). The solution of (P2), however, is physically realizable because it represents reacting segments (PFR's with residence times determined from P2) in series with separation units between them (see Figures 2a and 2b). This realization has actually been performed for the two example problems in section 6.

One important issue that still needs attention is the objective function. It is intuitively obvious that if a separation cost is not associated with it, we will usually end up getting near complete separations of products, and hence complete conversions to an extent possible within stoichiometric constraints. Thus the attainable region in concentration space can easily be the entire stoichiometric space. Unfortunately, to get an accurate representation for the separation cost is rather difficult, especially when sharp splits are not enforced. Here, we present a simple cost model by assuming that the variable cost of separation is determined by two factors, namely, the difficulty of separation and the mass flow rate through the separator.

We first consider an example for modeling the separation costs. As shown in the schematic below, a stream with components A,B,C and mass flow rates F_A, F_B, F_C undergo a separation operation into two output streams, with mass flow rates F_{A1}, F_{B1}, F_{C1} and mass flows $F^2, Fg \gg F C 2$ respectively. The streams A, B, and C are arranged in a sequential order of separability; for example, in the case of distillation, we may assume that A, B and C are in a decreasing order of volatility. The mass fractions $y_A, y_B,$ and $JQ,$ are then defined as: $y_A = F_{A1}/F_A, \quad \eta_B = F_{B1}/F_B - Y_C = F_{C1}/F_C$

If the split fractions $Y_A = Y_B = Y_C = 0$ * c n ** *s obvious that we only have a splitting operation without any separation. However, if they are not equal, then there is a relative separation between two adjacent components in the mixture. Given that the streams are arranged in a monotonic order of separability, we define, $|y_A - y_B|_0$ as a measure of the intensity of separation between the two components. When $Y_A \gg Y_B = Y_C = 0$ * we have only a splitting operation among these components, and the cost of separation is identically zero; whereas if $Y_A \gg Y_B = \pm 1$ we have a sharp split, between components A and B. Any intermediate degree of separation could then be modeled by complete sharp split separation followed by mixing, to achieve the desired composition.

In order to generalize this to formulate the separation costs, let $M = \{m\}$ denote the set of all components in the reacting system and let these be arranged in some monotonic order of relative separability, for example volatilities. If Q is the mass flow rate handled by the separator, then the cost of separation may be described by:

$$C_{sep} = C_{capital} + Q_{operating} \quad (24)$$

$$C_{capital} = C_{fixed} + \sum_{m;n=m+1} p_{mn} A_{Y_{mn}} Q \quad (25)$$

Here, y_{mn} is the binary variable associated with the separation of components m and n , such that if $y_{mn} = 0$, $A_{Y_{mn}} = 0$; and if $y_{mn} = 1$; $A_{Y_{mn}} \leq 1$. The second term in the above expression models the intensity of separation. Here, p_{mn} is a cost coefficient for unit separation between two adjacent components m and n and reflects the difficulty of separation between components m and n . Q is the net flow through the separation network. The above formulation gives us a reasonably accurate representation for sharp splits between adjacent components, i.e., $A_{Y_{mn}} = 1$. For nonsharp splits, there are two further options. First, the functional form of (25) assumes that the separation cost includes a fixed charge and is proportional to the feed flow rate multiplied by the degree of separation in that unit. Often, this is an adequate representation of separation costs; at least through appropriate choices of p_{mn} and C_{fixed} it can serve as a lower bound on these costs. On the other hand, an upper bound on nonsharp separation costs can be derived simply by enforcing $A_{mn} = 1$ in (27) whenever $y_{mn} = 1$ and thus modeling nonsharp splits by sharp splits followed by mixing.

Since we have binary variables, simple azeotropy or solubility constraints may be added without much difficulty into the optimization problem. For example, let $f(X) \geq 0$, be the azeotropy constraint which must be active whenever a separation is attempted between components m and n . (X is some subset of the variables in the problem). This can be written as:

$$f(X) \leq L(1 - y_{mn}) \quad (26)$$

where L is a suitable lower bound on $f(X)$. An example of these constraints is shown for the Williams-Otto problem in section 6. Finally, the operating cost (reboiler and

condenser duties in distillation, for example) can directly be incorporated into the energy minimization framework presented in the next section.

The presence of $I A_{mn} I$, in the cost function makes the objective function in P2 a non-differentiable one. However, this does not pose a problem since the cost function could be remodeled by adding the following constraints within P2.

$$\begin{aligned} \text{Max } J_{\text{exit}} &= J_{\text{product}}(m_c(\text{exit}), Q, \tau) + Q_{\text{fixed}}(mn) y_{mn} - \sum_{m;n=m+1}^{\infty} p_{mn} A_{mn} Q - \text{Cooperating} \\ \Delta_{mn} &\geq \gamma_m - \gamma_n \\ \Delta_{mn} &\geq \gamma_n - \gamma_m \end{aligned} \quad (27)$$

Since A_{mn} is to be minimized in the objective, it is easy to show that this reformulation would result in $A_{mn} = I A_{mn} I$, as we desired, at the optimal solution. Having addressed the nondifferentiability, the other question that now remains is the evaluation of p_{mn} . One of the ways to determine this would be through a nonlinear regression technique, where one could run several separation simulations based on sharp splits and get an approximate value of the parameter p_{mn} for particular systems. Here, the above separation targeting technique has been tested on the Williams-Otto flowsheet problem using different test values for the cost coefficients. This problem is also interesting due to the azeotropy constraints that exist in the system. The return on investment (ROI) is chosen as the objective function and a comparison between the results with and without the integration of the reactor with the flowsheet is presented in the examples section.

3. Unified Formulation for Optimal Energy Utilization

The combined reaction-separation model has its advantages in its ability to consider both reaction and separation within one framework. In this section, we extend this formulation to include energy minimization using concepts of energy targeting, so that the heat effects within the reactor are integrated optimally with the energy flows in the flowsheet. Heat integration involves the matching of heat loads between a set of hot and cold streams so as to minimize the cost of utilities for the network. However, the reacting streams cannot be classified *a priori*, because an optimal temperature trajectory within the reactor could be both nonlinear and nonmonotonic. To address this, we discretize the temperature profile within the reactor and use the concept of candidate

streams (Balakrishna and Biegler, 1992b). The optimal temperature trajectory in the reactor is approximated by a set of isothermal segments followed by temperature change between these segments as shown in Figure 4.

Here the horizontal lines correspond either to hot streams or cold streams depending on whether the reaction is exothermic or endothermic. The vertical sections may involve heating and cooling and therefore we assume the presence of both heaters and coolers between the reacting segments. Also, these streams are candidate streams because they may or may not be present in the optimal network, depending on the separation profiles within the network. Furthermore, both the heaters and the coolers before any reacting segment cannot be active simultaneously, since it would be suboptimal to heat and then cool the same stream. Figure 2b shows one finite element of the discretized reactor-separator representation of Figure 2a along with the candidate heat exchange streams.

The energy minimization scheme for this network follows the development for reactor networks in Balakrishna and Biegler(1992b). Here, we extend this formulation to optimize the reactor separation profile, while ensuring maximal energy integration. The discretized reactor separator model is integrated within an energy targeting framework based on minimum utility consumption (Duran and Grossmann, 1986). For energy targeting we consider only utility costs in the simultaneous synthesis procedure, as these often tend to be most directly affected when one considers integrated flowsheet optimization. On the other hand, capital cost targets can also be incorporated easily into the formulation given below, if required. Based on these assumptions, a unified reactor-separator-energy target can be derived from the solution to the following mixed-integer nonlinear programming problem:

$$\text{Max } T(GW, QH, QC) = J(GW) - CHQH - ccQcr C^p \quad (P3)$$

$$\text{s. t } S_k X_{ik} L_k^f(a_j) - R(Xy, Tij)A < Xi = 0 \quad j = 1, K \quad (28)$$

$$X(0) = X_0 \quad (29)$$

$$Xi_{end} = I_k X_{ik} L_k(t_{end}) \quad (30)$$

$$X^o F_i = (1 - Y_{c4-1}) X_{c,(H)end} F(i-1) \quad (31)$$

$$F_{c,exit} = S_i Y_{e1} X_{c(i)end} F_i \quad (32)$$

$$\Delta_{mn} \leq y_{mn} \quad (33)$$

$$0 \leq y_{mn} \leq 1 \quad (34)$$

$$\Delta_{mn} \geq Y_{in} - Y_n \quad (35)$$

$$\Delta_{mn} \geq Y_n - Y_{out} \quad (36)$$

$$Q_C = Q_H + \sum_{h \in H} W_h [T_h^{in} - T_h^{out}] - \sum_{c \in C} w_c [t_c^{out} - t_c^{in}] \quad (37)$$

$$Z_{HP}(\omega) = \sum_{c \in C} w_c [\max\{0; t_c^{out} - \{TP - \Delta T_{roJJ} \cdot \max\{t_{cinMTP}, \Delta T_m\}\}].$$

$$- \sum_{h \in H} w_h [\max\{0; T_h^{fa} - TP\} - \max\{0; T_h - \Delta T\}]. \quad (38)$$

$$Q_H \wedge Z_{HP}(V). \quad V \text{ pinch candidates } p \quad (39)$$

$$g(\omega, \psi, y) \leq 0 \quad (40)$$

$$h(\omega, \psi, y) = 0 \quad (41)$$

Here, the variables are defined as follows:

- ω : Set of variables in the reaction-separation-energy network
(Variables in Equations (28) to (39))
- ψ : Set of external flowsheet parameters
- Q_H, Q_C : Heating and Cooling utility loads
- C_H, C_C : Cost coefficient for utility loads
- W_H, W_C : Heat capacity flow rates for hot and cold streams respectively
- Q_{sep} : Total Separation Cost
- p : Pinch candidates, inlet temperatures of all cold and hot streams
- T_h^{in}, T_h^{out} : Inlet and Outlet temperatures respectively for hot stream h
- t_c^{in}, t_c^{out} : Inlet and Outlet temperatures respectively for cold stream c
- F_j : Total mass flow rate at element i .
- Z_{HP} : Heating deficit above the pinch for pinch candidate p

The objective function F , is a function of the variables within the unified reactor model, and the heating and cooling utility loads. The cost model for separation presented in the previous section is directly incorporated within F as C^p . The operating costs for the separation profile (for example, heat loads in the case of distillation) are directly incorporated into the energy minimization formulation. Equation (28) is the residual from the orthogonal collocation discretization for the rate equation within each finite element, similar to model P2. Equations (31) and (32) are the mass balance equations for the separation and the sum of bypasses leaving the reactor model. Equations (37) to (39) correspond to those in the energy minimization subsystem. Equation (37) is an energy balance for hot and cold streams with inlet temperature vectors given by Th^M and tc^{in} ; and outlet temperature vectors given by Th^{out} and tc^{out} , respectively. TP, the pinch candidate temperature, corresponds to combined vector of all the inlet temperatures for the hot streams, and $to^{in} + AT_m$ for all the cold streams. Equation (38) is the value of the heating deficit above every candidate pinch (Duran and Grossmann, 1986), where each candidate pinch given by TP. The minimum heating utility consumption is then given by the maximum of the ZHP values from (38). Thus equation (38) is of dimensionality of the total number of heat exchange streams. The heats of reaction are directly accounted for by the heat capacity flow rates of the reacting streams as follows. If QR is the heat of reaction to be removed (or added, for endothermic reactions) to maintain isothermality in the reacting segment, the equivalent $(FCp)h$ or Wh for this reacting stream is equated to QR, and we assume a 1 K temperature difference for this reacting stream. For pure condensing or boiling liquids within the separators, we again assume a 1 K temperature difference with an equivalent heat capacity set to the heats of vaporization. Equations (40) and (41) are the equations that bind the integrated reactor variables (j) with the rest of the flowsheet variables (co).

It is clear that the above formulation corresponds to a nondifferentiable mixed integer nonlinear program due to the presence of the max functions in (38). Here, we use the hyperbolic approximation function developed in Balakrishna and Biegler (1992b) to convert the above problem to a continuous nonlinear program. We approximate $\max(0,Z)$ as $\sqrt{Z^2 + e^2}/2 + Z/2$, where e is chosen to be sufficiently small ($e = 0.01$). The advantage in this representation is that it provides a single function approximation over the entire domain, unlike previous quadratic or exponential approximations. The solution to the resulting smoothed MINLP will determine the optimal exit flow distribution and temperature profiles for the reactor network, while simultaneously minimizing the utility consumption for the entire flowsheet

4 Model Simplification for Special Systems

The formulation above provides a general scheme for synthesizing energy integrated reaction-separation networks. However, for large flowsheets or complex reaction mechanisms, the non-linearities within this model can be severe. Especially, the smoothing of (38) results in an extremely non-linear set of $(NH + Nc)$ equations, where NH and Nc are the total number of hot and cold streams, respectively. Here, we investigate strategies to simplify this model for systems with substantially high reaction exothermicities. Typically, the heat content to be removed from the hot streams in the flowsheet is much higher than the energy content in the cold streams for highly exothermic reaction systems. A typical T-Q plot for such a system is shown in Figure 5.

The hot stream curves are relatively flat for such systems and much hotter than the cold streams over a long range, and the maximum hot and cold stream temperatures are the same. This is because, the maximum hot stream temperature for exothermic reactions is usually the temperature of the inlet stream to the reactor which is the same temperature at the exit from the preheater (the cold stream). It can be inferred from the T-Q plot that for such systems, the pinch point will correspond to the highest temperature of the hot stream, and the energy demand from a hot utility, which is very small, is equal to $F_{PHTR}AT_{min}$, where F_{PHTR} is the heat capacity flow rate of the cold stream in the preheater and AT_{min} is the minimum approach temperature. Also, since the hot stream curve is always above the cold stream curve, most of the cold streams which have relatively small heat content can be moved over a long range with the same minimum utility consumption. The width (or the heat content) of the hot stream at a higher temperature ensures that there is no temperature crossover. It follows then that for such cases, the pinch point is already predetermined. Therefore, the constraints (38) and (39), which are formulated to identify the pinch points can be omitted. Since Q_H is no longer evaluated from (39), the utility cost in the objective function is now reformulated from $CHQ_H + ccQ_c$ in P3 to the following expression:

$$C_{util} = CCEA[Q_C + F_{PHTR}AT_{min}] + CH[F_{PHTR}AT_{min}]$$

where, $AQ_C = Q_c - Q_H$ is the energy deficit, given by the energy balance equation in (37). This reformulation leads to substantial savings in the effort for solving the problem,

since it eliminates a large number of nonlinear constraints (and nonlinear nonzero elements) from the smoothing of (38). The optimization then only determines the optimal spread of the cold stream curves to achieve maximum heat integration. Example 2 illustrates the application of both formulation P3 and its simplification and the results indicate that similar profiles are obtained in both cases with substantial savings in computer effort for the simplified model.

5 Reactor Extensions

The solution to formulation P3 gives us an optimal network for the reactor flow configuration shown in Figure 1. However, this flow model may not be sufficient for the synthesis problem, and we need to check if there are any other reactors that will help us improve the objective function. The solution of P3, therefore, gives only a lower bound on the objective function for the synthesis problem. Using the constructive approach developed in Balakrishna and Biegler (1992b), we check for CSTR extensions from the solution to our unified reactor targeting model, because CSTR's lead to reasonably good targets and yield much smaller problems. In other words, we add a CSTR model to the targeting model of Figure 1, and solve P3 along with the CSTR extension to our model. This constitutes the addition of the following constraints in P3 in order to maximize $F^{(2)}$ instead of F .

$$\begin{aligned} \text{Max } r(2)(\langle D, \|K2\rangle, QH, Qc) &= J \ll M^{(2)} \rangle' CHQH - ccQc - Qep & \text{(P4)} \\ \text{[Constraints of P3]} & \\ X_{CSTR} &= X_{exit}^{(P3)} + R(X_{CSTR}, TCSTR) * CSTR \\ 0 \leq \tau_{CSTR} &\leq \tau_{max} \end{aligned}$$

Here, $Y^{(2)}$ is the set of new variables in the reactor energy network, which includes all the variables within y and the new variables X_{CSTR} , $TCSTR$ and X_{CSTR} with the corresponding heat exchange variables for cooling/heating the stream in the CSTR. There are no additional separation variables, since separation is confined to the segregated flow component of this system. $X_{exU}^{3\wedge}$ is the reactor exit concentration variable within model P3. If the optimal solution to this formulation $r^{(2)} * \xi T^*$, then we have a reactor extension that improves the objective function. The next step consists of creating the new convex hull of concentrations and checking if there are further extensions that improve the objective function within the flowsheet constraints. We continue this procedure until there are no further reactor extensions that improve the

objective function. However, for these systems, reactor extensions are less likely to be observed than for systems without reactive separation. This is mainly because the choice of separation already includes a large choice for the attainable region. The advantage with this scheme is that only the simplest model that is needed for the reaction system is solved.

6 Example Problems

In this section, we present two example problems to illustrate our synthesis approach. The first example illustrates the combined reaction-separation model for a reaction system, while the second example shows the application of the unified reaction-separation-energy integration model. Comparisons are made between sequential and simultaneous modes of synthesis, and the applicability of the simplified energy target model is also verified.

Example 1. Here, we consider the Williams and Otto flowsheet problem (Williams and Otto, 1960) which has been often studied as a typical flowsheet optimization problem. The schematic of the flowsheet for this problem is shown below.

The plant is to manufacture a chemical P and consists of a reactor, a heat exchanger to cool the reactor outflow, a decanter to separate a heavy byproduct G and a distillation column to separate product P. A portion of the bottom product is recycled to the reactor and the rest is used as fuel.

1. $A + B \rightarrow C$
2. $C + B \rightarrow P + E$
3. $P + C \rightarrow G$

The rate vector for components A,B,C,P,E,G respectively is given by,

$$R(X) = [-k_1 X_A X_B ; -(k_1 X_A + k_2 X_C) X_B ; 2k_1 X_A X_B - 2k_2 X_B X_C - k_3 X_P X_C ; k_2 X_B X_C - 0.5k_3 X_P X_C ; 2k_2 X_B X_C ; 1.5k_3 X_P X_C]$$

where, $k_1 = 6.1074 \text{ h}^{-1} \text{ wt fraction}$, $k_2 = 15.0034 \text{ h}^{-1} \text{ wt fraction}$, $k_3 = 9.9851 \text{ h}^{-1} \text{ wt fraction}$.

The X's here denote the weight fractions of the components. F_A , F_B are the flow rates of fresh A and B. F_Q is the flow rate of waste G and F_p is the fixed exit flowrate of pure P out of the plant. Traditionally, this problem has been solved previously by assuming the reactor to be an isothermal CSTR and optimizing the volume and temperature of this CSTR to maximize the return on investment. Here, we replace the CSTR with our reaction-separation targeting model of Figure 1. A flat temperature profile (isothermal system with temperature as variable) was assumed within the model. This model is now embedded within a global recycle, i.e.; the inlet conditions to this targeting model PI are now given by the recycle and the fresh feed flow rates. Included among the constraints in this system are the constraints in P2 and the mass balances at the global recycle. The order of volatilities in the system is given by the following descending order of [P,E,C,B,A]; G is a heavy by-product. Furthermore, component P forms an azeotropic mixture with component E, hence there is an azeotropy constraint in the system. The azeotropy constraint requires that whenever a separation between components P and E is attempted, an amount of P equivalent to at least 10 percent weight fraction of E is lost along with stream E. This can be modeled by:

$$F_{P[i+1,0]} \geq 0.1F_{E[i,Cnd]} - U(1-y_{iPE});$$

where,

- y_{iPE} : Binary variable denoting separation between P and E in element i
- $F_{P[i+1,0]}$: Mass flow of P entering finite element i+1
- $F_{E[i,Cnd]}$: Mass flow of E leaving finite element i

and U is a reasonably large positive number.

The objective function, namely the rate of return, includes all raw material and separation costs for the entire plant, and is given by the following expression:

$$J = [8400 (0.3F_P + 0.0068F_D - 0.02F_A - 0.03F_B - 0.01F_G - C_{sep}^{var}) - 0.124*8400 (0.3F_P + 0.0068F_D) - C^{\wedge} * * * ^1 - 2.22F_R] / (6F_{RX});$$

Here, F_R denotes the total flow of species within the reactor, F_D is the flow of byproducts from the distillation column that are used for fuel, x is the residence time within the reactor, C_{sq}^{var} and $C^{\wedge} * * * ^{\wedge}$ are the variable and fixed costs for separation, given by the expressions in (25) and (26).

In the discretization procedure, we used fixed collocation element lengths and restricted separation to occur only between elements. The following three cases were considered:

Case (a): Separation only after the reaction steps are completed: Here, reaction and separation are totally uncoupled and take place sequentially, precisely as described in the flowsheet. However, the CSTR is replaced by our reactor targeting model where all the $Y_{c,i}^f$'s are forced to be equal to each other, i.e; separation is turned off within the reactor. Since there is no separation during the reaction process, there are no binary variables and the problem just reduces to a non-linear program. A return on investment (ROI) of 130% has been typically obtained for this problem in the literature with the fixed CSTR model. With the reactor targeting model integrated within the flowsheet, a ROI as high as 278% was obtained, thus indicating that significant savings can be obtained by integrating the reactor with the flowsheet, even with very simple models. Here the optimal reactor network is given by a single plug flow reactor with a residence time of 0.0111 h. This is the same case described and detailed in Balakrishna and Biegler (1992a).

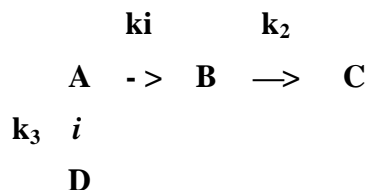
Case (b). Separation allowed during reaction : Here, we embed the complete reactor-separator targeting model and allow simultaneous reaction and separation. The formulation now is a mixed integer nonlinear program due to discrete decisions involved in the separation at different ages within the model. The azeotropy constraints should be active only if there is a separation between P and E in the midst of the reaction. DICOPT++ (Viswanathan and Grossmann, 1990) was used to solve the resulting optimization problem from the application of model P2. All of the optimization models were formulated within the GAMS modeling system (Brooke et al., 1988) Because the separation costs associated with detailed designs can vary over a wide range, we present the following two cases to demonstrate the sensitivity to separation costs. We expect more detailed simulations to follow these trends qualitatively as well.

(i) $C_{fixd}(mn) = \$200000$, per separation attempted between any two components m and n, and the separation cost coefficient of Equation (26), $p_{mn} = 0.0001$. In this case, we observe a very high ROI of 1027% and the optimal network indicates a key separation between components C and (EP) ($A_{ycE} > 0$) with components P, E and G going to the reactor exit as shown in the Table I below. The optimization model (223 constraints, 230 variables) was solved in 295.57 sees on a VAX 6320. The separation profile indicates P,

E, and G leaving the reactor, which agrees with intuition, since G is a waste by-product with significant penalties and removal of P curbs the production of G. No further CSTR extensions that improve the objective function are observed for this system. Also, the mean residence time was 0,009 hrs and the reactor network is shown in the Figure 7. Note that at each separation node in Figure 7, there are two sharp splits involved; the first one between components PE and C, the second between component A and component G.

(ii) In this case the cost coefficient p_y was increased 50 times to 0.005. Here, the optimal network indicated no separation within the reactor, since the raw materials were not expensive enough to warrant the high separation costs. The optimal ROI was therefore the same as in case (a), namely 278%, where we have a reactor without any separation profile followed by the distillation as columns shown in Figure 6.

Example 2 . For this process we consider a gas phase reaction that follows Van de Vusse kinetics, with a reaction diagram as shown below. This mechanism is typical in several industrial processes, such as propylene chlorination.



where,

$k_{10} = 8.86 \times 10^6 \text{ h}^{-1}$, $k_{20} = 9.7 \times 10^9 \text{ h}^{-1}$, $k_{30} = 9.83 \times 10^3 \text{ lit-mol}^{-1} \text{ h}^{-1}$; and

$E_1 = 15.00 \text{ kcal/gmol}$, $E_2 = 22.70 \text{ kcal/gmol}$ and $E_3 = 6.920 \text{ kcal/gmol}$

$\Delta H_{A \rightarrow B} = -0.4802 \text{ kcal/gmol}$, $\Delta H_{B \rightarrow C} = -0.918 \text{ kcal/gmol}$ and $\Delta H_{A \rightarrow D} = -0.792 \text{ kcal/gmol}$.

Here, we seek to devise a reaction separation network featuring energy integration for this system using the proposed targeting scheme. The feed to the plant consists of pure A. This is mixed with the recycle gas stream consisting of almost pure A, and preheated (C1) before entering the reactor. The flowsheet in Figure 8 shows the reaction separation network followed by final separation columns to obtain product streams containing pure

B and a C-D mixture. The volatility of components in the network are given in the following descending order: [A,B,C,D]. The distillation columns are assumed to operate with a constant temperature difference between reboiler and condenser temperatures (Andrecovich and Westerberg, 1985) and can operate over various pressure levels. The reflux ratios are assumed fixed and the column temperatures are functions of the pressure in the column, which is variable so that efficient heat integration can be attained between the distillation columns and the rest of the process. The operating costs of the distillation columns (reboiler and condenser duties) are directly incorporated into the energy integration formulation. The reactor here is modeled by the discretized targeting model as shown in Figure 5, with 8 finite elements in the collocation procedure. The discretization procedure results in a total of 18 candidate hot streams and 11 candidate cold streams within the reaction separation network. The objective here is to maximize the total profit given by:

$$J = 30F_B - 18F_{CD} - 6.95 \times 10^{-4} x_1^4 - 4.566 F_A (1 + 0.010 x_1^{15} - 320) - 7(F_B + F_{CD}) - 2F_{A0} - C_{sep} - 0.07Q_C - 0.8Q_H$$

In this expression, F_B , F_{CD} represent the production rates of B and CD respectively. F_{A0} is the amount of fresh feed. The first term corresponds to the product value, while the second term corresponds to the cost of waste treatment for undesired products C and D. The third term corresponds to the reactor capital cost, while the fourth and the fifth terms correspond to the recycling costs. C_{sep} denotes the costs incurred for maintaining a desired separation profile and is given by Equation (25). The operating costs of the columns are directly incorporated into the energy network in terms of condenser and reboiler heat loads. We assume that the cost of the reactor can be described by the total residence time and is independent of the type of reactor. This can be justified on the grounds that the capital cost of the reactor itself is often much smaller than the operating costs and the capital costs of the downstream processing steps. A target production rate of 960000 lb/day is assumed for the desired product B. Here, we consider two alternatives. Firstly, we consider the sequential reaction and separation approach, where we force all the separation fractions to only split fractions. In the second case, we solve the above problem with the formulation proposed in P3. Here, the reactive-separation system and the energy network are optimized simultaneously. Table II and Figures 9 and 10 present a comparison between the results obtained for simultaneous reactive separation and sequential reaction and separation.

The results clearly show that by considering simultaneous reaction and separation as an option within the network, significant increases in overall profit can be obtained for this system. As shown in Figure 9, the separation profiles indicate removal of B and CD as reaction progresses, while retaining A for the complete residence time of 0.45 sees. The temperature profile is a falling one as long as B and CD remain in the reactor. At every point where B and CD are separated out of the reactor, the temperature rises. This is because as long as there is only A, a high reaction rate is desired to minimize reactor volume, however as more B is produced the temperature profile falls so as to reduce the excessive degradation of B to product C. Thus the optimal temperature profile in this case is a non-monotonic one. Also among the 8 finite elements used in the discretization, only the candidate streams corresponding to 6 elements are active, since at the end of the sixth element, all molecules leave to the reactor exit ($t=0.45$ sees), as shown by the separation profile in Figure 9. Furthermore, of the eighteen candidate hot streams and eleven candidate cold streams, only twelve hot streams and six cold streams were active in the optimal network. Also, from the solution of the reactor extension problem (P4) no reactor extensions are observed that improve the objective function for both sequential and simultaneous formulations.

An energy analysis shows that the temperature enthalpy curve for this system follows the criteria for substantially exothermic reactions. The simultaneous formulation is again applied to this system by using the simplification for such systems as described in Section 3. Table HI presents a comparison of the results obtained by solving the complete model P3 and the simplified model derived from P3, for the simultaneous case. The results clearly show that the targets derived are nearly the same in terms of utility costs and the overall profit function, while the reduction in computer effort is significant. Thus the simplified model is sufficient for deriving targets for this system. Even if the exothermicity conditions are not satisfied, the solution to the simplified model provides a good starting point. Note that once the flow patterns and the temperature profiles are known, the HEN network can easily be synthesized with available tools (e.g., MAGNETS, Floudas et al, 1986). Also, the network is innately flexible since the cold streams can be moved over a long range of the T-Q curve for the same minimum utility consumption.

Conclusions

The examples clearly show the advantages of simultaneously considering reaction, separation, and energy management within one framework. Even though there have been previous efforts in integrating process subsystems, reaction and separation were always considered as sequential processes within the flowsheet. This work is a first step in analyzing simultaneous reaction and separation as an option within a flowsheet. The formulation is developed from a simple choice of a species dependent residence time distribution, the optimization of which leads to a separation profile along the length of the reactor. The first example illustrates that depending on the relative ratio of the separation costs to the raw material costs, the reactor network can change from a plug flow reactor (PFR) to a PFR with a separation profile shown in Table I.

The accurate evaluation of the separation costs can be difficult for many systems. This, however, does not pose a serious problem, since the targeting approach can still be applied by using bounds on the separation costs. As mentioned above, in the general case of non-sharp splits, lower and upper bounds on the separation costs can be derived. By applying the formulation P3, with both the lower and upper bounds on the separation costs, we can assess the importance of separation in the course of reaction. Clearly, if the solution with a lower bound on the separation costs indicates that separation is non-optimal in the course of reaction, we can infer that for this system, separation during the process of reaction is non-optimal even with the actual costs. Again, if we find separation to be optimal during the course of reaction, with an upper bound on the separation costs, we can infer that reactive separation could be an attractive option in the actual case with realistic costs. With such a bounding analysis, the importance of separation in the course of reaction can be evaluated.

The amalgamation of this formulation with an energy minimization scheme leads to a more powerful tool for preliminary design. While previous work (Glavic et al. , 1988) has considered only the case of adiabatic or isothermal systems with sequential reaction and separation, here, we allow any optimal temperature profile within the reactor. This is accomplished through the concept of candidate streams, which are required to match the optimal temperature profile within the reactor. Example 2 illustrates the application of this targeting model for a system with Van de Vusse kinetics. For the separation costs considered, the optimal solution indicates that B, C, D are separated out to the reactor exit. This is intuitively justified, since there are penalties on producing excessive C and D. Furthermore, the cooling costs and reactor volume are also lowered due to the smaller flow rates within the reactor network. The results also show that for substantially exothermic reactions a simpler model can be solved in much

less time. For large synthesis problems, even if the exothermicity conditions are not completely satisfied, this simplification could yield reasonably good initial targets. It must be noted, however that most reactor synthesis problems are highly nonlinear and global optimality cannot usually be guaranteed. However, the sequential bounding scheme leads to a robust solution procedure since relatively simple optimization problems are solved with monotonically improving objectives. The main strength of the constructive approach is that only the simplest model that is needed is solved, and reactor extensions are generated only when they are required

APPENDIX A: RTD FOR THE SEPARATION TARGETING PROBLEM

Here, we derive the residence time distribution for the seg flow model with separation.

Let $f(\alpha)$ be the true residence time distribution of the molecules within the reactor network. We know then that if $Q(\alpha)$ is the flow rate at any age α , then:

$$Q(\alpha) = Q_0(1 - F(\alpha)) \quad (\text{A-1})$$

where $F(\alpha)$ is the cumulative distribution function = $\int_0^{\alpha} f(t)dt$

In the model with separation we have,

$$\frac{dQ}{d\alpha} = -Z_c \frac{V_c(X)m_c(\alpha)}{\rho}$$

$$Q(0) = Q_0$$

The solution of this gives :

$$Q(\alpha) = Q_0 - Z_c \int_0^{\alpha} f Y_c(a) q_c(a) da \quad (\text{A-2})$$

where $\hat{C}_a = m_c(\alpha)/\rho$

Equating the right hand sides of (A-1) and (A-2) and rearranging, we get

$$F(\alpha) = \sum_c \frac{\gamma_c(\alpha) q_c(\alpha)}{Q_0}$$

Differentiation of this integral gives:

$$f(\alpha) = \sum_c \frac{\gamma_c(\alpha) q_c(\alpha)}{Q_0}$$

which gives the actual residence time distribution function for this system.

If $\gamma_c(\alpha)$ is independent of component c , then

$$f(\alpha) = \gamma_c(\alpha) \sum_c \frac{q_c(\alpha)}{Q_0} = \gamma_c(\alpha) \frac{Q(\alpha)}{Q_0}$$

$$\Rightarrow f(\alpha) = \gamma_c(\alpha)(1-F(\alpha))$$

$$\Rightarrow \gamma_c(\alpha) = \frac{f(\alpha)}{1-F(\alpha)}$$

Thus, given one distribution function it is easy to get the other and thus get an expression for the mean residence time.

APPENDIX B: Proof for Discretization Equivalence

We need to prove that the nonlinear programming formulation, P2 is equivalent to the original optimal control problem PI in the limit as the length of the finite elements goes to zero. The differential mass balances, in the reacting model PI are given by:

$$X_{c,\alpha+\delta\alpha} Q_{\alpha+\delta\alpha} - X_{c,\alpha} Q_{\alpha} =$$

$$R_c(X,T) Q_{\alpha} \delta\alpha - Y_{c,a}^* Q_{\alpha} X_{c,\alpha} \quad (B-1)$$

$$Q_{\alpha+\delta\alpha} = Q_{\alpha} \left(1 - \frac{\sum_c \gamma_{c,a}^* X_{c,\alpha}}{\rho} \right) \quad (B-2)$$

(B-1) can be rewritten as the following set of equations (see Figure B -1):

$$X_{a+8a}Q_{a+5a} - X'_{a+5a}Q_{a+5a} = R(X,T)Q_{a+8a} \quad (\text{B-3})$$

$$X'_{c,a}Q_{a+5a} = \gamma_{c,a}Q_{a+5a} - \gamma_{c,a}X_{c,a} \quad (\text{B-4})$$

Equations (14-16) correspond to a particular choice for (B-3), while Equation (17) corresponds exactly to Equation (B-4), where $\gamma_{c,a} = y^*$. Since (B-3) and (B-4) are equivalent to (B-1) and (B-2), it is enough to show that (B-1) corresponds to the original model (PI)

Therefore, substituting (B-2) for the value of Q_{a+5a} into (B-1), we get:

$$[X_{c,\alpha+\delta\alpha} - X_{c,\alpha}] - X_{c,\alpha+\delta\alpha} \frac{\delta\alpha}{\rho} = R_c(X,T)\delta\alpha - \gamma_{c,\alpha}X_{c,\alpha}$$

Dividing by $\delta\alpha$ and taking the limit as $\delta\alpha \rightarrow 0$, we get;

$$\frac{d}{da} [X_{c,\alpha} + X_{c,\alpha} \rho] \left[\frac{\gamma(\alpha)^T X(\alpha)}{\rho} - \gamma_c(\alpha) \right]$$

whereas $\delta\alpha \rightarrow 0$, $\rho \rightarrow Y_a$

The above differential equation is the same as the governing equation for the reaction-separation model, and hence as $\delta\alpha \rightarrow 0$, the equivalence is proved

Acknowledgements

Support for this work from the Engineering Design Research Center, an NSF sponsored center at Carnegie Mellon University is gratefully acknowledged

References

Andreovich, M. J., and A. W. Westerberg, "An MILP Formulation for Heat Integrated Distillation Sequence Synthesis," (1985) *AIChE J.*, 31, p. 363

Balakrishna, S. , and Biegler, L. T. , " A Constructive Targeting Approach for the Synthesis of Isothermal Reactor Networks", (1992a) *Ind. Eng. Cham. Research*, 31(1), 300

Balakrishna, S., and Biegler, L. T., " Targeting Strategies for the Synthesis and Energy Integration of Nonisothermal Reactor Networks", (1992b) *Ind. Eng. Chem. Research*, 31(9), 2152

Brooke, A., D. Kendrick, and A. Meeraus, "GAMS: A User's Guide," (1988) Scientific Press, Redwood City, Calif.

Cuthrell, J. E., and L. T. Biegler, " On the Optimization of Differential Algebraic Process Systems," (1987) *AIChE J.* , 33,1257

Douglas, J. M., " A Hierarchical Decision Procedure for Process Synthesis", (1985) *AIChE J.*, Vol 31, pp. 353 - 362.

Douglas, J. M. *Conceptual Design of Chemical Processes*. (1988) McGraw-Hill Book Company, New York, NY.

Douglas, J. M, " A Hierarchical Decision Procedure for the Synthesis of Complex Plants," (1989) *Foundations of Computer Aided Process Design*, Snowmass, Col.

Duran, M. A., and Grossmann, I. E., "Simultaneous Optimization and Heat Integration of Chemical Processes", (1986) *AIChE J.*, 32,123 .

Floudas, C. A., A. R. Ciric and I. E. Grossmann, "Automatic synthesis of optimum heat exchanger network configurations," (1986) *AIChE J.*, 32, p. 276

Glasser, D. , C.Crowe and D.Hildebrandt, " A Geometric Approach to Steady Flow Reactors: The Attainable Region and Optimization in Concentration Space", (1987) / & *EC research*, 26(9),p.1803

Glavic, P., Kravanja, Z, and Homsak, M., "Heat Integration of Reactors -1. Criteria for the Placement of Reactors into the Flowsheet", (1988) *Chem. Eng. Sci.*, Vol. 43,3,593

Glavic, P., and Bikic, D., "Computer Aided Process Synthesis for Complex Reactions" *European Federation of Chemical Engineering*, (1988) XIX Conference, Chemdata 88, Goteborg, Sweden.

Kokossis, A.C and C.A.Floudas, "Synthesis of Isothermal Reactor-Separator-Recycle Systems" 1989 *Annual AIChE meeting*, San Francisco, CA

Pibouleau, L., J. Floquet, and S.Domenech, "Optimal Synthesis of Reactor Separator Systems by Nonlinear Programming Method," (1988) *AIChE Journal*, 34, p163 (1988)

Vasantharajan, S. and L.T. Biegler, "Simultaneous Strategies for Parameter Optimization and Accurate Solution of Differential Algebraic Systems, " (1990) *Computers and Chemical Engg.* 14 (8), p 1083 (1990)

Viswanathan, J. V. and Grossmann, I.E., "A Combined Penalty function and outer-approximation method for MINLP optimization," (1990) *Comput. and Chem. Engg.*, 14, 769-782

Williams, T, J., and R. E. Otto, "A generalized chemical processing model for the investigation of computer control," (1960) *Trans. IEE*, 79, p. 458

Nomenclature

c	: Index set of components in the reaction system
$c_{H>C}$: Cost coefficient for utility loads
C	: Total number of components in reaction system
C_{sep}	: Cost associated with a separator
f	: Residence time distribution
F_i	: Total mass flow rate at element i .
J	: Objective function for synthesis
$Lk(oc)$: Lagrange interpolation polynomial of degree k
$Lk^f(x)$: Derivative of the Lagrange interpolation polynomial
m_c	: Mass flow of component c
$mc(exit)$: Mass flow of component c at reactor exit
$mc(0)$: Mass flow of component c at reactor entry
P_{mn}	: Cost coefficient for unit separation between two components m and n
QfQ_0	: Volumetric flow rate and flow at reactor entry respectively
$QH>QC$: Heating and Cooling utility loads
R	: Reaction Rate Vector
T	: Temperature
T_{CSTR}	: Temperature in CSTR
T_h^{in}, T_h^{out}	: Inlet and Outlet temperatures respectively for hot stream h
t_c^{in}, t_c^{out}	: Inlet and Outlet temperatures respectively for cold stream c
$w_H>w_C$: Heat capacity flow rates for hot and cold streams respectively
X_{ik}	: Mass concentration vector in the discretized model
X_{iend}	: Mass concentration at the end of element i
X_0	: Concentration vector at reactor entry
X_{CSTR}	: Concentration at exit of CSTR extension
X_{exit}	: Mass concentration at reactor exit
$y_{m,n}$: Binary variable denoting separation between components m and n
z_H^P	: Heating deficit above the pinch
Greek Letters	
V	: Set of variables in the reaction-separation-energy network
CD	: Set of external flowsheet parameters
a	: Age within reacting environment

Y : Species split fraction vector (array of Y_c)
p : Density
F : Objective function for unified model Pf3

Figure 1. Flow model for combined reaction-separation targeting

Figure 2a, Finite Element Discretization for Reaction-Separation targeting model

Figure 2b: Discretized model for energy minimization

Figure 3. Illustration for separation mass fractions

Figure 4: Optimal trajectory approximation

Figure 5 T-Q plot for typical exothermic systems

Figure 6 Flowsheet for Williams-Otto Reaction-Separation Synthesis

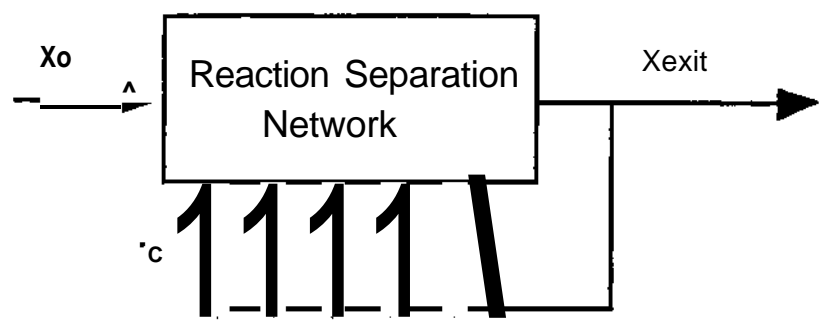
Figure 7. Reactor module for Williams - Otto Flowsheet

Figure 8. Flowsheet for Reaction-Separation Synthesis with Energy Integration

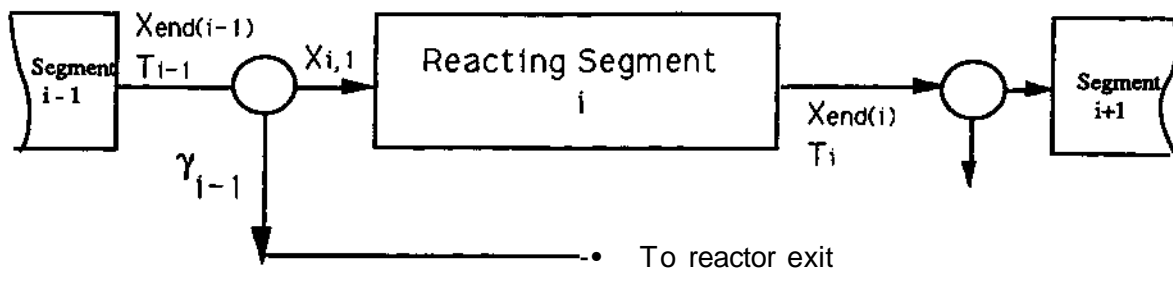
Figure 9 Separation profiles along reactor length (Simultaneous Case)

Figure 10 Temperature Profile (Simultaneous Case)

Figure B-1. Reactor Discretization

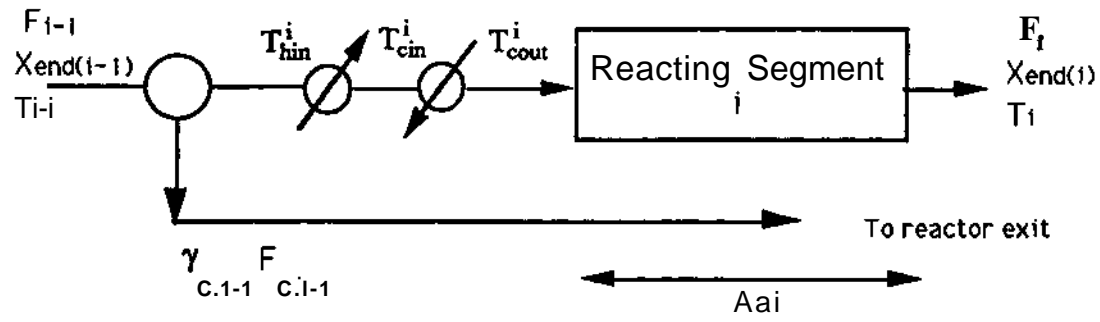


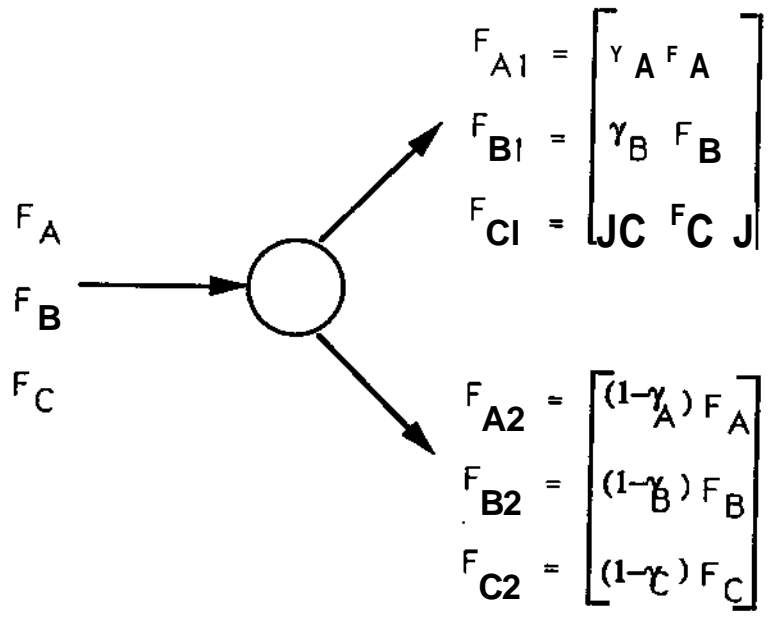
3a



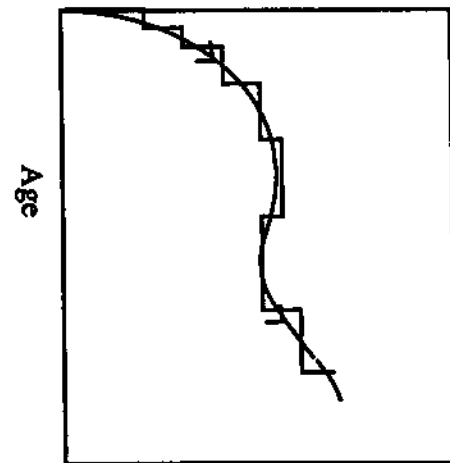
O → Separator / Splitter

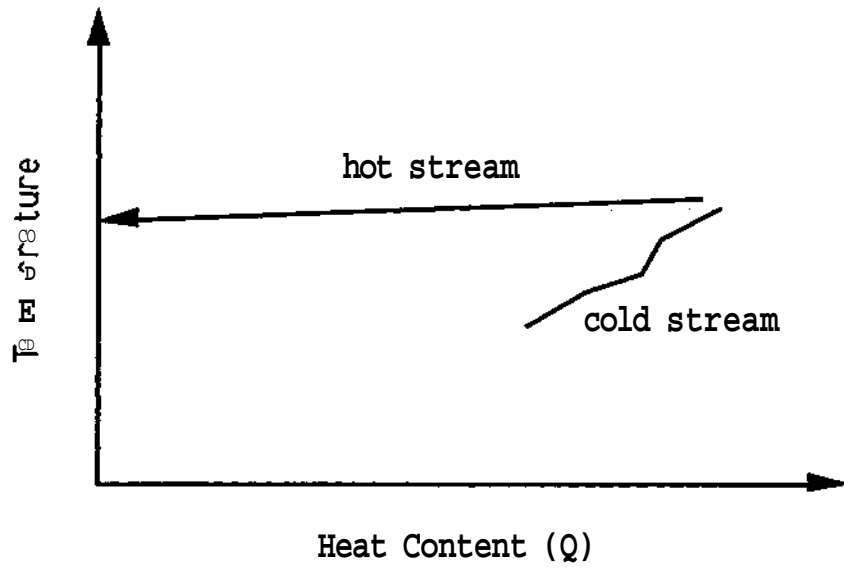
26

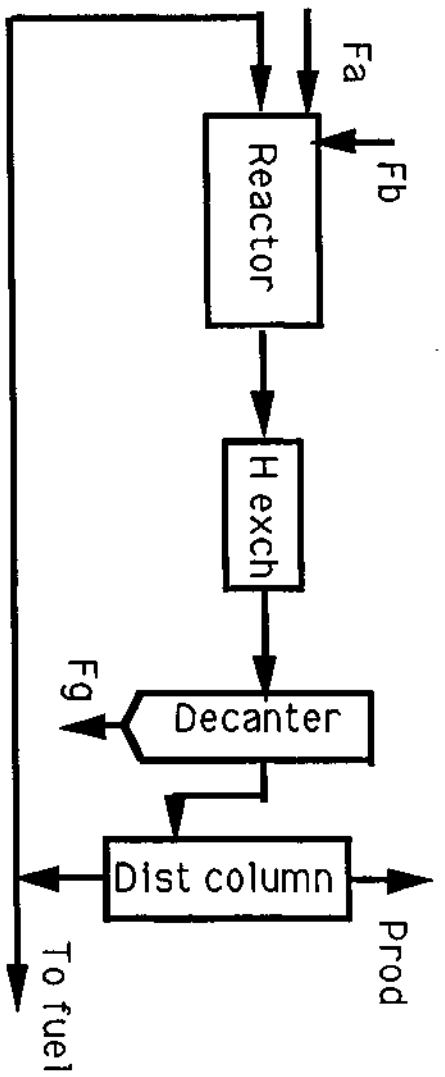


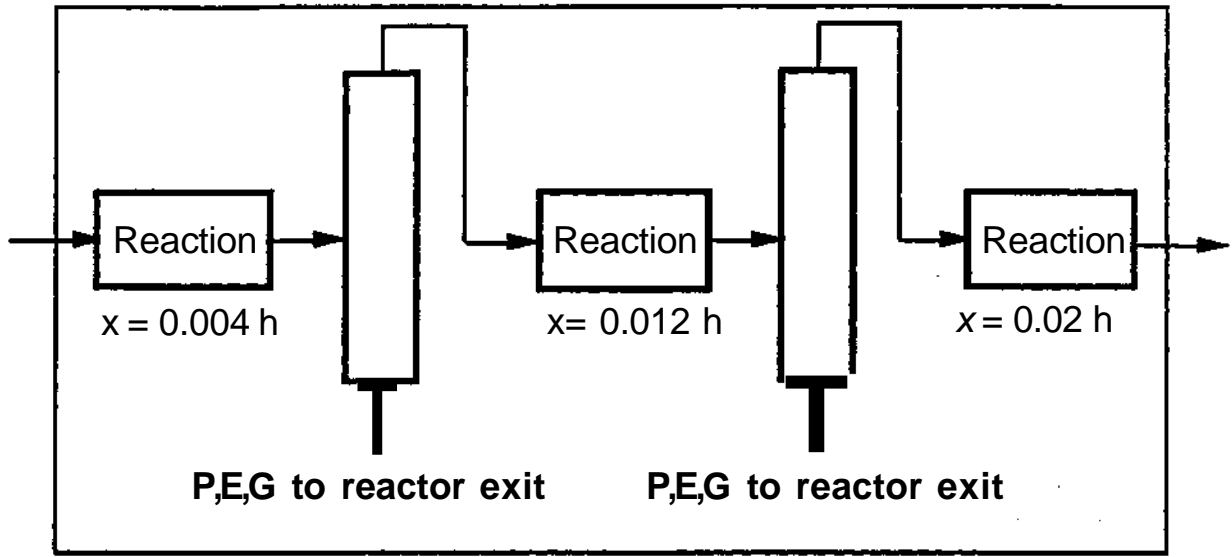


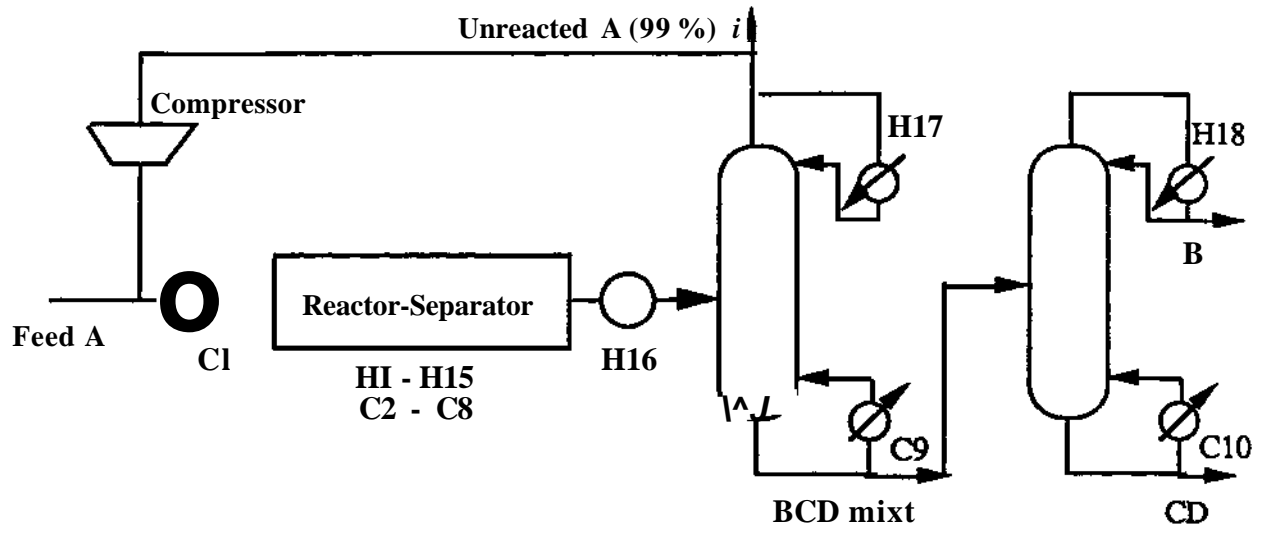
Temperature

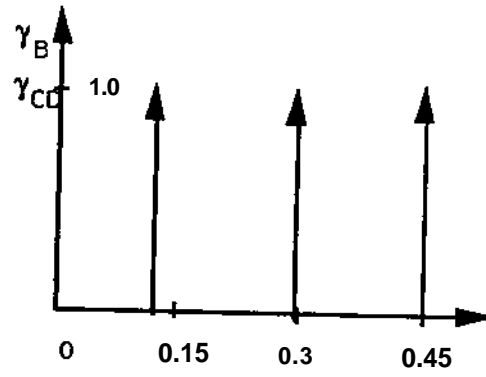
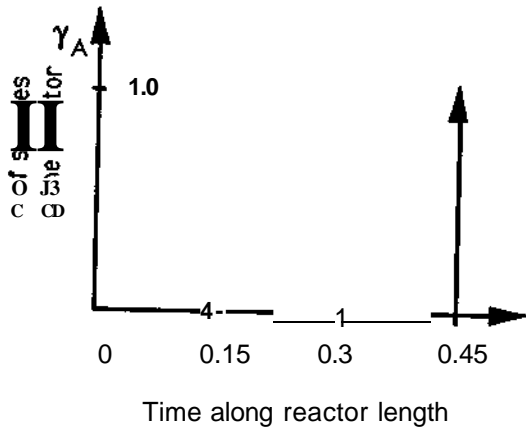


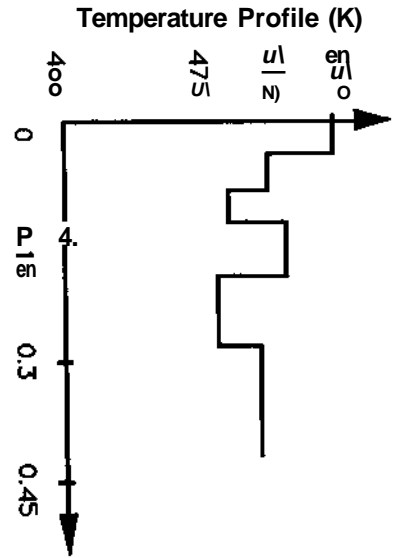


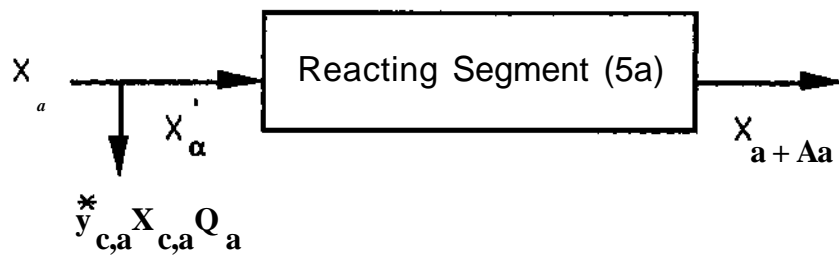












Age within targetting model (hrs)	Fraction of P,E,G to join reactor exit
0.004	1.00
0.012	1.00

Table I. WDIams-Otto Example - Case b(i)

	Sequential Reaction and Separation model	Simultaneous Reactive separation model
Overall Profit	53.87 x 10 ⁶ \$/yr	202.33 x 10 ⁶ \$/yr
Hot utility load	3.20 x 10 ⁵ BTU/hr	2.13 x 10 ⁵ BTU/hr
Cold utility load	131.120 x 10 ⁶ BTU/hr	126.799 x 10 ⁶ BTU/hr

Table II. Results for sequential and simultaneous formulations

	Complete Model	Simplified Model Solution
Overall Profit	202.33 x 10 ⁶ \$/yr	202.23 x 10 ⁶ \$/yr
Hot utility load	2.13 x 10 ⁵ BTU/hr	2.3 x 10 ⁵ BTU/hr
Cold utility load	126.799 x 10 ⁶ BTU/hr	126.82 x 10 ⁶ BTU/hr
Variables	792	703
Constraints	820	703
CPU time (Vax 6320)	239 sees	133 sees

Table DDL Comparison between rigorous and simplified model solutions